Geophysical Research Letters

RESEARCH LETTER
10.1029/2020GL091538

Key Points:

- Natural pseudotachylyte-filled shear zones can reactivate plastically at high temperature
- Plastic deformation processes are dominated by diffusion creep at low temperatures
- Rheology of pseudotachylytes can reduce the strength of the continental crust

Supporting Information:

- Supporting Information S1

Correspondence to:
F. X. Passelègue,
passelegue@gmail.com

Citation:
Passelègue, F. X., Tielke, J., Mecklenburgh, J., Violay, M., Deldicque, D., & Di Toro, G. (2021). Experimental plastic reactivation of pseudotachylyte-filled shear zones. *Geophysical Research Letters*, *48*, e2020GL091538. https://doi.org/10.1029/2020GL091538

Received 2 NOV 2020
Accepted 15 FEB 2021

Experimental Plastic Reactivation of Pseudotachylyte-Filled Shear Zones

François X. Passelègue[1], Jacob Tielke[2], Julian Mecklenburgh[3], Marie Violay[1], Damien Deldicque[4], and Giulio Di Toro[5]

[1]Laboratoire de Mécanique des Roches, École Polytechnique Fédérale de Lausanne, Lausanne, Switzerland, [2]Lamont-Doherty Earth Observatory of Columbia University, Palisades, NY, USA, [3]SEES, The University of Manchester, Manchester, England, [4]Laboratoire de Géologie de l'École Normale Supérieure, Paris, France, [5]Dipartimento di Geoscienze, Università degli Studi di Padova, Padua, Italy

Abstract Pseudotachylytes are fine-grained fault rocks that solidify from melt that is produced in fault zones during earthquakes. Exposed sections of natural fault zones reveal evidence of postseismic plastic deformation (i.e., reactivation) of pseudotachylyte, which suggests these rocks may contribute to aseismic slip behavior in regions of repeated seismicity. To measure the plastic flow behavior of pseudotachylyte, we performed high-temperature deformation experiments on pseudotachylyte from the Gole Larghe Fault Zone, Italy. Plastic reactivation of pseudotachylyte occurs at temperatures above 700°C for strain rates accessible during laboratory experiments. Extrapolation of experimental results to natural conditions demonstrates that pseudotachylyte deforms via diffusion creep at crustal conditions and is much weaker than host rocks in seismically active regions. Importantly, the presence of plastically deforming pseudotachylyte may influence the thickness of the seismogenic layer in some fault zones that experience repeated seismicity.

Plain Language Summary While the plastic strength of individual minerals constituting the continental crust are well known, the plastic strength of rocks resulting from coseismic slip in seismically active regions has yet to be measured, despite of the observations of their plastic reactivation. Here, we establish the flow law parameters controlling the strength of natural pseudotachylyte, fine-grained fault rocks that crystalize from melt produced in fault zones during earthquakes. Experiments where conducted at temperature ranging from 700 to 900°C and at a confining pressure of 300 MPa. Our experimental results demonstrate that pseudotachylyte deforms via diffusion creep at crustal conditions. Flow law parameters derived from plastically deforming pseudotachylyte suggest that the presence of pseudotachylyte along faults drastically reduces the strength of the seismically active continental crust. Finally, the presence of seismically generated pseudotachylyte is likely to strongly influence the thickness of the seismogenic layer, since seismicity is rare in mature crustal faults at depths below which pseudotachylyte deforms plastically.

1. Introduction

The seismogenic layer spans the range of depths within the crust at which most earthquakes nucleate and propagate (Brace & Byerlee, 1970; Scholz, 1998). The thickness of this layer varies at different locations, and is expected to be controlled by (a) the composition and thickness of the crust (from ~40 to 60 km and from ~10 to 25 km for continental and oceanic crust, respectively) (Watts & Burov, 2003), (b) the age of the crust (Jackson et al., 2008), and (c) the geodynamic context of the area (Figure 1a). The lower boundary of the continental seismogenic zone is limited by the onset of crystal-plastic deformation of minerals constituting the crust at depth. The strength of the continental crust for semibrittle to ductile deformation is commonly modeled using the laboratory measurements of the strength of quartz and feldspars (Hirth & Tullis, 1994; Hirth et al., 2001; Rybacki et al., 2006; Tullis & Yund, 1992) while the oceanic crust is modeled using the strength of dolerite (diabase) and basalt (Darot et al., 1985; Kohlstedt et al., 1995; Violay et al., 2012). These experimental studies highlighted that at a given strain rate, the bottom of the seismogenic zone is mostly controlled by the activation of plastic deformation processes, such as dislocation and diffusion creep, which become more active with increasing temperature (Darot et al., 1985; Hirth et al., 2001; Kohlstedt et al., 1995; Rybacki et al., 2006). In addition, experimental studies also demonstrated that grain size sensitive creep

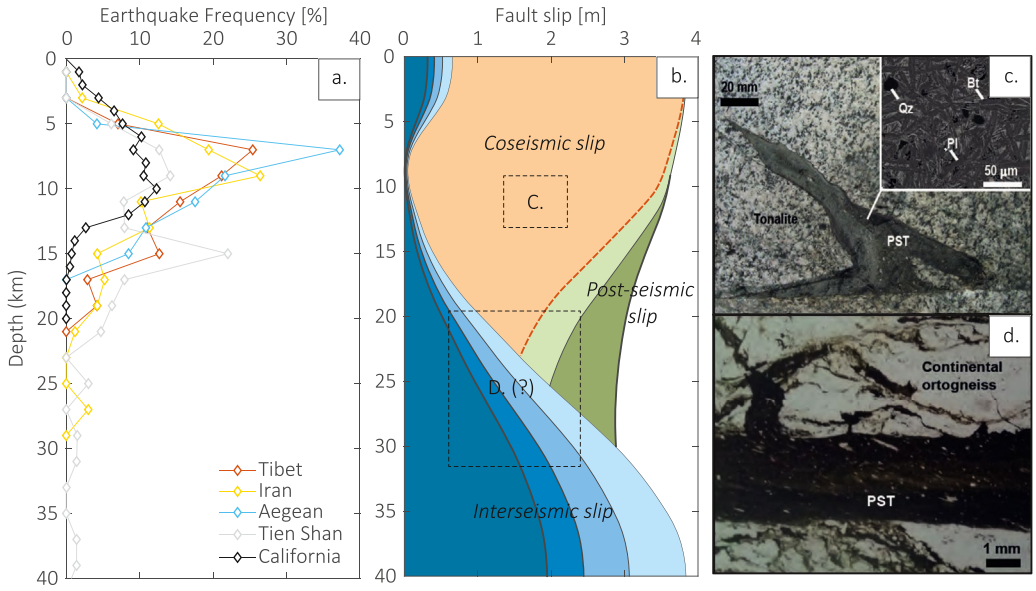

Figure 1. Geological context of the study. (a) Distribution of the seismicity and thickness of the continental seismogenic layer of Earth (Jackson et al., 2008). (b) Illustration of the deformation history within the continental crust]during the seismic cycle (modified from Tse and Rice [1986] and Handy and Brun [2004]). Here, the rupture nucleates at a depth of 7–8 km and propagates down to a depth of 22 km. Seismic rupture propagation (orange in color) in the middle crust is arrested by the limited elastic strain energy available in the plastically deforming crust. Stress relaxation drives postseismic deformation in the middle to deep crust (green in color). The different shades of colors correspond to successive time windows. Boxes c and d are typical crustal depths where fault rocks shown in figures (c) and (d) can be found. (c) Field picture of pseudotachylyte-bearing (PST) fault network hosted in tonalites (Gole Larghe Fault Zone, Adamello Massif, Italy). Top right image: microstructure of the pseudotachylyte with clasts of quartz (Q) suspended in a matrix of plagioclase (Pl) and biotite (Bt) microlites (Back Scatter Scanning Electron Microscope image). (d) Crystal-plastic deformation of pseudotachylyte fault vein hosted in continental granitic orthogneiss (Roraima, Brazil; optical microscope image, plane polarized light) (Trouw et al., 2009).

involves both diffusion and grain boundary sliding (Kronenberg & Tullis, 1984). Finally, recent studies highlighted the role of partial melting (Mecklenburgh & Rutter, 2003) and the presence of glass (Violay et al., 2012) in controlling strain localization and the strength of the crust (Jaroslow et al., 1996; Kirby, 1985; Platt & Behr, 2011). Understanding the physical processes that control the depth of the seismogenic zone is of great importance because the strength of the crust is also largely involved in controlling the earthquake cycle, from the nucleation of instabilities to the propagation of the seismic rupture. Earthquakes are the fast release of energy accumulated in the brittle crust (seismogenic layer) due to the large strain accommodated at depth by ductile mechanisms (Figure 1b).

While most of the rupture propagates within the seismogenic layer, coseismic slip affects the deformation behavior at the base of the seismogenic transition zone. The relic of coseismic slip within the brittle-ductile transition zone is highlighted by the presence of pseudotachylytes (solidified friction induced melts) in fault zone rocks exhumed from beneath the seismogenic zone (Figure 1c) (Goodwin, 1999; Menegon et al., 2017; Passchier, 1982; Pennacchioni & Cesare, 1997). In addition, the largest amount of displacement after an earthquake likely occurs within the zone that comprises the brittle plastic transition (Figure 1b) (Handy & Brun, 2004; Reilinger et al., 2000; Wright et al., 2013), which may explain the crystal-plastic reactivation of pseudotachylytes bearing rocks observed in nature (Figure 1d) (Goodwin, 1999; Menegon et al., 2017; Passchier, 1982; Pennacchioni & Cesare, 1997). Despite all of these observations, the onset of the crystal-plastic reactivation of pseudotachylyte as well as the implications of their presence at depth on the strength of the crust remains unknown (Rabinowitz et al., 2011). To address these issues, we present the results of creep experiments conducted on natural pseudotachylytes under high pressure and high-temperature conditions. This study aims to address the following questions: Under what conditions do pseudotachylytes

veins plastically deform? How does the presence of pseudotachylytes affects the hypocentral depth of earthquakes and the strength of the continental crust?

2. Experimental Setup

The samples used in this study are from the Gole Larghe Fault Zone which cuts the tonalites of the Adamello Massif, Italian Southern Alps (Di Toro et al., 2006). Three types of rocks were used in deformation experiments: (a) tonalite, which corresponds to the host rock of the fault zone, (b) cores made entirely of pseudotachylyte, and (c) tonalite containing tabular veins of pseudotachylyte oriented at 45° to the direction of maximum compressive stress (Figures S1 and S2a). The tonalite samples have grain size of 1–5 mm and are made of plagioclase (49%), quartz (29%), biotite (17%), and K-feldspar (6%) (Di Toro & Pennacchioni, 2004). The pseudotachylytes formed during faulting events at 9–11 km in depth and 250–300 °C ambient temperature (Di Toro & Pennacchioni, 2004).

The pseudotachylytes samples used in the experiments consist of (a) parent clasts of quartz and feldspar that survived from elevated temperatures during frictional melting and (b) microlites (up to 300 μm in length) of plagioclase and biotite that crystallized from the friction melt. Both parent grains and microlithes are suspended in an ultrafine matrix made of cryptocrystalline ($\ll$1 μm) grains of plagioclase and biotite. Pseudotachylytes often include small amounts subreenschist facies alteration minerals (mainly epidote) precipitated after frictional heat has dissipated (see Di Toro & Pennacchioni, 2004) for a complete description of the altered pseudotachylytes studied). While these altered pseudotachylytes are not expected to present exactly the same rheology than the fresh one made of amorphous glass, a recent study highlighted that alteration processes in greenschist facies can occur within months only after their formation (Fondriest et al., 2019). Because of the rapid onset of alteration, studying the rheology of altered pseudotachylytes is relevant to constrain the strength of active faults in the continental crust.

All experiments were conducted using an internally heated Paterson Instruments Ltd (Figure S1a) gas-medium apparatus (Paterson, 1990) at a confining pressure of 300 MPa. Individual samples of the three different starting materials were deformed at 700, 800, and 900°C. The samples were cored to make cylinders of 9.5 mm in diameter and 22 mm in length, which were placed between ceramic pistons inside of an iron jacket. An internal load cell was used to measure differential stress with a resolution of 0.5 MPa after correction of jacket strength contribution. Temperature was measured during deformation using a thermocouple placed in the hollow upper loading piston 3 mm from the top of the sample (Figure S1b). Based on thermocouple specification (Type K thermocouple) and furnace calibration, specimen temperature is believed to be accurate within ±7° along the sample length.

Once the target temperature was reached, a series of increasing constant force steps were applied and the resultant changes in displacement in response to the applied force was recorded (Figure S2a). The data recorded from the internal load cell and measured from LVDT (Linear Variable Differential Transformer) were combined with the sample dimensions to calculate the stress and strain rate for each force step. The stress data were corrected for the load supported by the iron jacket using the corresponding flow laws (Frost & Ashby, 1982). Strain data were corrected from the shortening of the sample length for experiments conducted on intact samples. No correction was applied for sample containing tabular veins of pseudotachylyte, because no variation in the vein thickness was observed on the postmortem sample. For each load step, the average strain rate was computed over a given time window interval. The representative strain rate data resulting from a creep step at a given differential stress were collected at steady state (Figures S2b and S2c).

3. Experimental Results

Our limit in sample diameter allows only for studying a rock sample containing 10–15 grains. Because of that, our estimates of the strength of the intact tonalite may vary from sample to sample, depending on whether plagioclase-rich, quartz-rich, or biotite-rich tonalite regions were cored. However, successful experiments on tonalite were carried out at 800 and 900°C. Experiments were attempted at 700°C, but required too large applied stresses to deform via crystal-plastic deformation for resolvable laboratory strain rates. At 800°C, stress steps ranging from 120 to 249 MPa yielded axial strain rates of 1.1×10^{-6} to

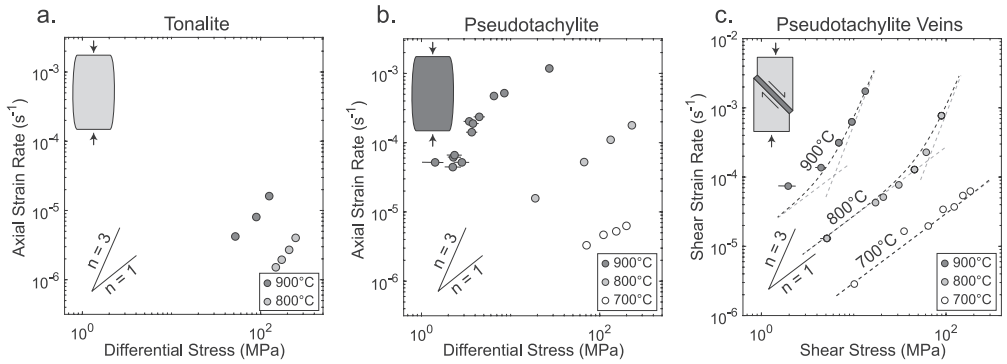

Figure 2. Mechanical data from creep experiments performed on tonalite (a), intact pseudotachylyte (b), and tabular pseudotachylyte veins (c). White, gray, and black circles correspond to experiments conducted at 700, 800, and 900°C, respectively. The dashed gray lines in figure c are the flow laws for diffusion ($n = 1$), dislocation ($n = 3$) creep. The black dashed line is a combination of the two mechanisms for the three investigated temperatures (see supporting information). Note that c is plotted as shear stress and strain rate not differential stress and axial strain rate.

4×10^{-6} s^{-1} (Figure 2a). At 900°C, stress steps ranging from 54 to 130 MPa yielded strain rates of 1.5×10^{-6} to 1.5×10^{-5} s^{-1} (Figure 2a). At these conditions, the strain rate dependence on stress follows a power-law relationship with a stress exponent (n) of ≈3 (Figure 2a).

Samples made entirely of pseudotachylyte were deformed at 700–900°C. At 700°C, stress steps ranging from 70 to 200 MPa yielded strain rates of 3.5×10^{-6} to 6.5×10^{-6} s^{-1} (Figures 2a and 2b). Intact pseudotachylyte deformed at 800°C and at stress steps ranging from of 20 to 231 MPa yielded strain rates of 1.6×10^{-5}–1.8×10^{-4} s^{-1}. At 900°C, the strength of the material becomes very weak, with stress steps ranging from 1.2 to 28.1 MPa yielding to strain rates ranging from 4.5×10^{-5} to 1.1×10^{-3} s^{-1} (Figure 2b). These results demonstrate that pseudotachylyte is much weaker than the host rock. However, while a stress exponent (n) of three was observed for the intact tonalite, the results obtained on intact pseudotachylytes reveal a variable exponent of ~1 at 700 and 800°C, which varies further at 900°C. This variation in the stress exponent could be due to our estimates of the strain rate that are not taking into account for strain localization occurring in the sample, and due to the fast strain rate that approaches the limit of the apparatus for the largest stresses tested.

At 700°C, pseudotachylyte veins sustained stresses ranging from 10 to 184 MPa, yielding to shear strain rates ranging from 2.8×10^{-6} to 6.5×10^{-5} s^{-1}. At these conditions, the strain rate dependence on stress follows a power-law relationship with a stress exponent (n) of 1 (Figure 2c). At 800°C, pseudotachylyte veins sustained stress steps ranging from 4 to 90 MPa, yielding to shear strain rates ranging from 1.2×10^{-5} to 7.5×10^{-4} s^{-1}. Note that, at this temperature, the highest shear stresses deviate from Newtonian behavior, consistent with an increase of the stress exponent from 1 to ~3 (Figure 2c). At 900°C, the pseudotachylyte vein becomes very weak and its plastic behavior does not follow a regular power-law relationship. Moreover, the pseudotachylyte vein sustained a maximum stress step of only 11 MPa, yielding to a strain rate of 1.2×10^{-3} s^{-1} (Figure 2c), highlighting the relative weakness of the sheared vein. Plastic reactivation of tabular pseudotachylyte veins was observed at all the investigated temperatures. These results suggest that pseudotachylyte veins are weaker than the host tonalite and that their presence promotes strain localization.

4. Postdeformation Microstructures

To further understand the deformation processes occurring during the plastic reactivation of pseudotachylytes, we performed scanning electron microscope (SEM) and electron backscatter diffraction (EBSD) analysis on intact pseudotachylyte, and pseudotachylyte veins from experiments conducted at 800 and 900°C. SEM analysis on intact pseudotachylytes revealed localized plastic deformation in experiments conducted at 800°C (Figure 3a). In weakly deformed regions, pseudotachylyte included domains of randomly oriented plagioclase (medium gray in color), microlitic rods with fine inclusions of biotite (white in color), wrapping

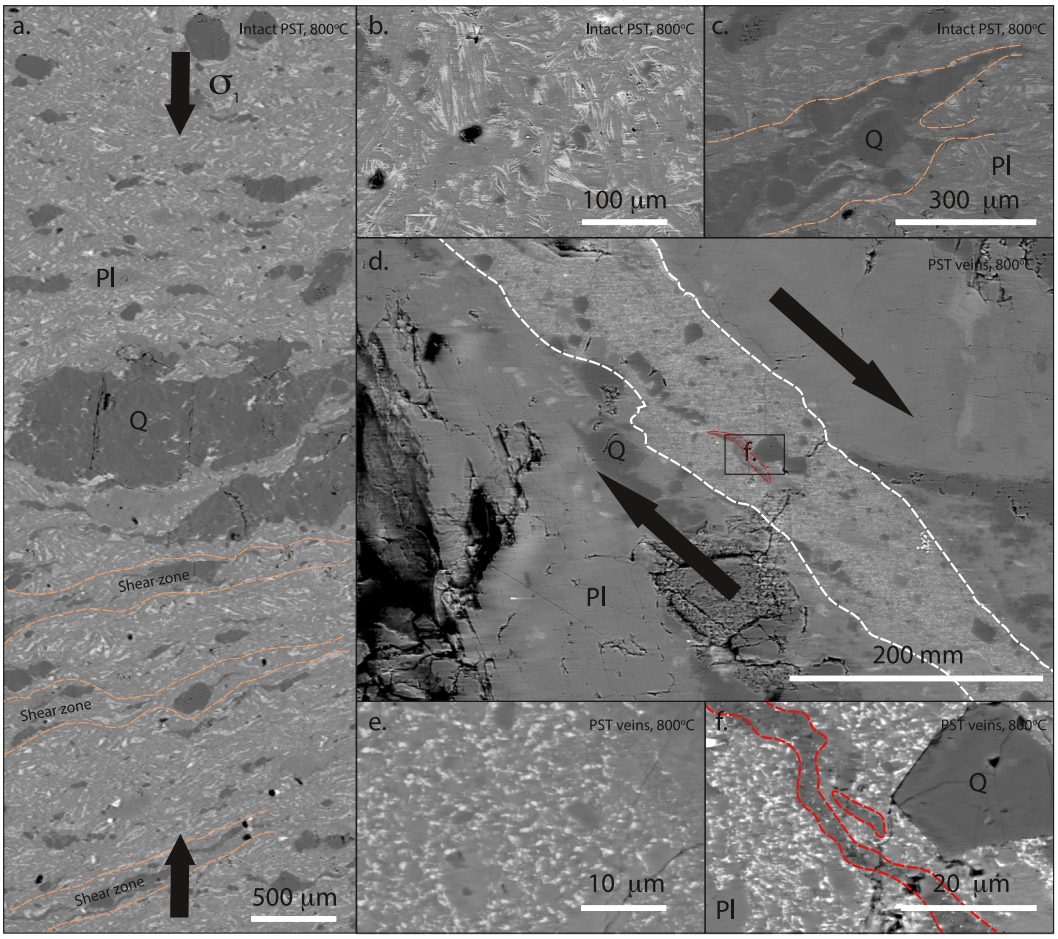

Figure 3. Backscattered electron images of plastically deformed pseudotachylyte-bearing rocks (Q, Quartz; Pl, Plagiolcase). (a) Pseudotachylyte after experiments conducted at 800°C. Black arrows indicate the orientation of the maximum stress. (b) Microstructures in pseudotachylytes after small strain which are similar to those observed in the starting material (Figure 1c). (c) Evidence of sigma-type tail development around quartz porphyroclasts assisted by partial melting and recrystallization. (d) Pseudotachylyte veins after experiments conducted at 800°C. Black arrows indicate the direction of shear. (e) Typical microstructures observed within the tabular pseudotachylyte veins after the experiment. No strong evidence of strain is observed. (f) Higher magnification image of the area in (d), with an outline of a melt-bearing pocket observed after experiment conducted at 800°C.

quartz (black in color), and plagioclase clasts that survived frictional melting (Figure 3b). These domains are typical of the starting natural pseudotachylyte (see Figure 4a in Di Toro and Pennacchioni [2004]). However, the high strain domains included reoriented microlitic rods (their long axes are subparallel to each other) of plagioclase and glassy-like pods suggesting the occurrence of localized melting during the highest temperature experiments (Figure 3c). In these areas, EBSD analyses indicate that only plagioclase grains have a crystallographic preferred orientation (Figure S4c), likely due to rotation to a stable orientation during shearing. These results suggest that while the reduced strength of the intact pseudotachylytes compared to the tonalite results in the activation of plastic deformation, the strain rates obtained at 900°C are affected by the presence of melt.

Analyses of pseudotachylyte veins highlight that the strain is accommodated within the veins and the host tonalite remains undeformed (Figure 3d). The grains constituting the recrystallized pseudotachylyte reveal very little evidence of recrystallization and crystal-plastic (i.e., dislocation) processes (Figure 3e) despite the veins sustaining a large finite strain ($\gamma = 5$). To understand the mechanisms allowing the reactivation of tabular pseudotachylyte veins, we conducted EBSD analysis within the veins on grains of quartz and feldspar. Neither exhibit any crystallographic preferential orientation (Figure S5). These results are consistent

with the mechanical data obtained and suggests that the dominant mechanism allowing the reactivation of the pseudotachylyte veins consists probably in diffusion creep processes. This result is opposed to the observation made in intact pseudotachylytes, where deformation seems to be related to the formation of a CPO by rotation of the feldpars. This difference can be related to the presence of melt in intact pseudotachylytes, that helps for feldspars rotation. In pseudotachylyte veins, isolated domains with glassy-like structures similar to those shown in Figure 3c were found in the samples sheared at 800 and 900°C. However, based on the scarcity of glassy-like structures, we infer that the amount of melt produced in the shear zone during these high-temperature experiments was low (melt fraction smaller than 1% of surface area). Importantly, the melt pockets are not interconnected and strain is not localized along the pockets (Figure S6), indicating that melting cannot influence the observed mechanical behavior in experiment on pseudotachylyte veins, as it might does for mechanical results obtained at 900°C in intact pseudotachylytes.

5. Estimation of the Flow Law Parameters for the Plastic Reactivation of Pseudotachylyte

To extrapolate our experimental data and compare them to previous works conducted on other rheologies composing the continental crust, we attempt to derive the flow law parameters for the for the plastic reactivation of pseudotachylytes from the Gole Larghe Fault Zone (Di Toro et al., 2006). Such kind of constitutive law describes deformation of rocks by a single mechanism (Kohlstedt et al., 1995). These largely empirical laws are often derived from monomineralic materials, with or without the contributions of water or grain size dependence. Because of that, the flow law presented in the following is expected to be representative only of the strength of fault zone filled by altered pseudotachylytes layer formed from granitic wall rock, presenting similar grain size distribution (Di Toro et al., 2006; Kirkpatrick & Rowe, 2013).

Only experimental data obtained on pseudotachylyte veins were used to extrapolate our results to a larger range of geophysical conditions. For this purpose, we solved our experimental results for flow law parameters by minimizing the sum of the residuals using a least-squares method. We focused on the experimental data obtained from tabular pseudotachylyte veins because the strain is localized only within the veins, and the deformation is more uniform than in intact samples. Experimental data suggest an increase of the stress exponent n from 1 to ~3 with increasing shear stress (Figure 2c). This increase can be explained by the transition from diffusion to dislocation creep processes (Hirth & Kohlstedt, 1995). The total shear strain rate ($\dot{\gamma}_{total}$) of pseudotachylyte veins were fit by using a constitutive equation consisting of two independent mechanisms, diffusion, and dislocation creep, following:

$$\dot{\gamma}_{total} = \dot{\gamma}_{diff} + \dot{\gamma}_{disl}, \tag{1}$$

where $\dot{\gamma}_{diff}$ and $\dot{\gamma}_{disl}$ have a power-law dependence on stress and an Arrhenius dependence on temperature. Therefore, $\dot{\gamma}_{diff}$ and $\dot{\gamma}_{disl}$ are equations of the form

$$\dot{\gamma} = A\,\tau^{n} \exp\left(\frac{-Q}{RT}\right), \tag{2}$$

where τ is the shear stress in MPa, A is an empirically derived constant, Q is the activation enthalpy in kJ/mol, R is the gas constant, and T is the temperature in K. The values of A and Q for $\dot{\gamma}_{diff}$ were determined by performing a fit to the data at 700°C and to the four lowest stress data at 800°C while fixing $n = 1$. The values of A, n, and Q for $\dot{\gamma}_{disl}$ were determined by performing a fit to the entire data set using the combined flow law for $\dot{\gamma}_{total}$ with the results of the fit for $\dot{\gamma}_{diff}$.

This procedure yielded the following relationships for plastically deforming pseudotachylyte

$$\dot{\gamma}_{diff} = 10^{3.8\pm1.6}\,\tau^{1} \exp\left(\frac{-193 \pm 32\ \text{kJ / mol}}{RT}\right)\text{s}^{-1} \tag{3}$$

and

$$\dot{\gamma}_{disl} = 10^{28.6\pm3.2}\,\tau^{3.4\pm0.4}\exp\left(\frac{-793\pm82\ \text{kJ / mol}}{RT}\right)\text{s}^{-1}. \quad (4)$$

The results of the least-squares fit are in excellent agreement with the measured mechanical behavior as exemplified in Figure 2c. Following our inversion, the activation enthalpy for diffusion creep is much smaller than for dislocation creep.

6. Implications and Discussion

Previous studies reporting experiments conducted at room temperature suggested that pseudotachylytes produced in the shallow (≤12-km depth) continental crust could induce an increase of the postslip strength of faults (Proctor & Lockner, 2016), inhibiting further shear on the same slip surface (Mitchell et al., 2016). This strengthening is explained by the welding of the slip surface during melt quenching (Di Toro & Pennacchioni, 2004). Conversely to these observations, our experimental results demonstrate that deeper in the continental crust (a) crystal-plastic reactivation of pseudotachylytes is systematically observed in the range of pressure and temperature tested (Figure 3) and (b) pseudotachylytes are much weaker than the host rock (Figure 2).

Our experimental results are in agreement with the crystal-plastic reactivation of pseudotachylyte-bearing rocks observed in nature (Figure 1d) (Goodwin, 1999; Menegon et al., 2017; Passchier, 1982; Pennacchioni & Cesare, 1997). While the finite strain achieved during experiments remains relatively small compared to natural cases, experiments conducted on intact pseudotachylytes at temperature ≥800°C highlight initiation of mylonitization processes, with notably the deformation-induced shape preferred orientation of feldspar as well as the development of wings on porphyroclasts composed of recrystallized quartz and feldspar (Figures 3a and 3c). However, little evidence of crystal-plastic deformation is observed in the pseudotachylyte veins samples compared to the initial material because diffusion creep is the dominant mechanism operating during crystal-plastic reactivation of pseudotachylytes veins.

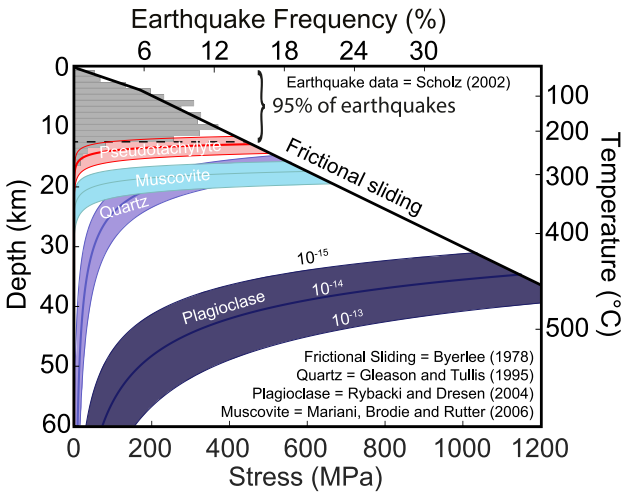

Figure 4. Extrapolation of our experimental results to natural conditions assuming an equivalent strain rate ranging from 10^{-15} to 10^{-13} s^{-1}. The geothermal gradient was computed from heat flux measurements (McKenzie et al., 2005). The frictional sliding criteria assumes regular friction criteria (Byerlee, 1978). Earthquake data represented by gray bars correspond to Californian seismicity (Scholz, 2002). The flow laws for wet quartz (Gleason & Tullis, 1995) and plagioclase (Rybacki & Dresen, 2004) are described by the blue domains, where each solid lines corresponds to a different strain rate (10^{-15}, 10^{-14}, and 10^{-13} s^{-1}). The experimentally determined flow law for diffusion creep of pseudotachylyte is represented by the red curves and domain. The transition from frictional sliding to diffusion creep of pseudotachylytes is predicted to occur at a similar depth as the deepest recorded earthquakes.

While results obtained from experiments conducted on intact pseudotachylytes highlight the weakness of the material, partial, and very local melting (glassy-like pods) at the contact between biotite and quartz is observed in samples from experiments conducted at 900°C. At this highest temperature, partial melting could be at the origin of the enhancement of the strain rate. However, this is not the case for tabular pseudotachylyte veins at 700 and 800°C. Only small and not interconnected regions with minor glass are observed, suggesting that local melting does not contribute to strain accommodation and localization. These results suggest that the reactivation of pseudotachylyte veins is controlled by plastic processes and, based on the lack of crystallographic preferred orientation in quartz and feldspar, mostly by diffusion creep. The weakness of the tabular pseudotachylytes, as well as the derived flow law parameters for diffusion creep, depends on the grain size of the material. Variation in grain size even of tens of microns, as well as the presence of water, could have a significant effects on the rheology of the material (Hirth et al., 2001; Tokle et al., 2019). However, most of the altered pseudotachylytes observed along natural faults present similar highly dispersive grain sizes distribution, with a matrix composed of very fine grains and, in rare cases, relics of melt (Kirkpatrick & Rowe, 2013).

Extrapolating our experimentally derived flow law for diffusion creep of pseudotachylyte to natural conditions gives insight into the strength of the continental crust in actively deforming regions. Assuming common geologic strain rates (10^{-14} s^{-1} (Kohlstedt et al., 1995) and geothermal

gradient for continental crust, respectively (Jackson et al., 2008; McKenzie et al., 2005)), our experimental results demonstrate that the brittle to crystal-plastic transition of pseudotachylyte-bearing rocks occurs at shallower depth than for coarse-grained quartz and feldspar. Note that because the experiments were conducted on natural samples, we were not able to constrain the grain size dependence on the diffusion creep flow law used here to extrapolate our experimental results to natural observations. The extrapolation presented here is only valid for fault zone filled with the same material, that is, altered pseudotachylytes resulting from the melting of granitic rocks presenting similar grain size distribution. However, our results are consistent with a recent synthesis of data from experiments on quartz, which predicts fast plastic deformation rates of fine-grained material at conditions near the brittle-ductile transition in Earth's crust (Tokle et al., 2019).

Our results suggest that if the strain rate and the geothermal gradient chosen are well constrained, the behavior of pseudotachylyte may constrain the upper-limit of seismicity depth in some natural fault zones (Figures 1a and 4). The presence of pseudotachylyte within fault zones could reduce the strength of the crust, and locally control the transition from brittle to plastic deformation. These results are in agreement with the crystal-plastic reactivation of pseudotachylytes bearing rocks observed in nature (Figure 1d) (Goodwin, 1999; Menegon et al., 2017; Passchier, 1982; Pennacchioni & Cesare, 1997). These new results suggest that the rheology of rocks generated during earthquakes could limit the thickness of the seismogenic layer in some fault zones that experience repeated seismicity (Figure 4), and their low strength could explain the large earthquakes after slip within the brittle crystal-plastic transition (Figure 1b) (Handy & Brun, 2004; Reilinger et al., 2000; Wright et al., 2013).

Data Availability Statement

The additional data to reproduce the figures presented in this study are given in the supporting information. Raw data are available can be found on the Zenodo repository under deposit (https://zenodo.org/record/4543476#.YCvTki17Q6g).

Acknowledgments
F. X. Passelègue acknowledges the Swiss National Science Foundation Grant PZENP2/173613, G. Di Toro and F. X. Passelègue the ERC Grant 614705 NOFEAR and J. Mecklenburgh and J. Tielke the NERC Grant NE/M000087/1. Authors thank experimental officer Stephen May for assistance with specimen fabrication and equipment maintenance, and Dr. Mark Zimmerman for assisting with designing high-temperature furnaces. Authors thank T.M. Mitchell for initial experiments conducted on synthetic pseudotachylytes. This work benefits from invaluable discussions with E. Rutter. Authors thank an anonymous reviewer during a first round of review for his enthusiasm regarding our work. Authors thank Andrew Cross and an anonymous reviewer for their constructive reviews. Raw data are available can be found on the Zenodo repository under deposit (https://zenodo.org/record/4543476#.YCvTki17Q6g).

References

Brace, W., & Byerlee, J. (1970). California earthquakes: Why only shallow focus? *Science*, *168*(3939), 1573–1575.
Byerlee, J. (1978). Friction of rocks. *Pure and Applied Geophysics*, *116*, 615–626. https://doi.org/10.1007/BF00876528
Darot, M., Gueguen, Y., Benchemam, Z., & Gaboriaud, R. (1985). Ductile-brittle transition investigated by micro-indentation: Results for quartz and olivine. *Physics of the Earth and Planetary Interiors*, *40*(3), 180–186.
Di Toro, G., Hirose, T., Nielsen, S., Pennacchioni, G., & Shimamoto, T. (2006). Natural and experimental evidence of melt lubrication of faults during earthquakes. *Science*, *311*(5761), 647–649.
Di Toro, G., & Pennacchioni, G. (2004). Superheated friction-induced melts in zoned pseudotachylytes within the Adamello tonalites (Italian Southern Alps). *Journal of Structural Geology*, *26*(10), 1783–1801.
Fondriest, M., Mecklenburgh, J., Passelegue, F., Artioli, G., Nestola, F., Spagnuolo, E., & Toro, G. D. (2019). Pseudotachylytes alteration and their loss from the geological record. *Geophysical research Abstracts*, *21*.
Frost, H. J., & Ashby, M. F. (1982). *Deformation mechanism maps: The plasticity and creep of metals and ceramics*. Oxford, UK: Pergamon Press.
Gleason, G. C., & Tullis, J. (1995). A flow law for dislocation creep of quartz aggregates determined with the molten salt cell. *Tectonophysics*, *247*(1–4), 1–23.
Goodwin, L. B. (1999). Controls on pseudotachylyte formation during tectonic exhumation in the south mountains metamorphic core complex, Arizona. *Geological Society, London, Special Publications*, *154*(1), 325–342.
Handy, M., & Brun, J.-P. (2004). Seismicity, structure and strength of the continental lithosphere. *Earth and Planetary Science Letters*, *223*(3–4), 427–441.
Hirth, G., & Kohlstedt, D. L. (1995). Experimental constraints on the dynamics of the partially molten upper mantle: Deformation in the diffusion creep regime. *Journal of Geophysical Research*, *100*(B2), 1981–2001.
Hirth, G., Teyssier, C., & Dunlap, J. W. (2001). An evaluation of quartzite flow laws based on comparisons between experimentally and naturally deformed rocks. *International Journal of Earth Sciences*, *90*(1), 77–87.
Hirth, G., & Tullis, J. (1994). The brittle-plastic transition in experimentally deformed quartz aggregates. *Journal of Geophysical Research*, *99*(B6), 11731–11747.
Jackson, J., McKenzie, D., Priestley, K., & Emmerson, B. (2008). New views on the structure and rheology of the lithosphere. *Journal of the Geological Society*, *165*(2), 453–465.
Jaroslow, G., Hirth, G., & Dick, H. (1996). Abyssal peridotite mylonites: Implications for grain-size sensitive flow and strain localization in the oceanic lithosphere. *Tectonophysics*, *256*(1–4), 17–37.
Kirby, S. H. (1985). Rock mechanics observations pertinent to the rheology of the continental lithosphere and the localization of strain along shear zones. *Tectonophysics*, *119*(1–4), 1–27.
Kirkpatrick, J. D., & Rowe, C. D. (2013). Disappearing ink: How pseudotachylytes are lost from the rock record. *Journal of Structural Geology*, *52*, 183–198.

Kohlstedt, D., Evans, B., & Mackwell, S. (1995). Strength of the lithosphere: Constraints imposed by laboratory experiments. *Journal of Geophysical Research*, *100*(B9), 17587–17602.
Kronenberg, A. K., & Tullis, J. (1984). Flow strengths of quartz aggregates: Grain size and pressure effects due to hydrolytic weakening. *Journal of Geophysical Research*, *89*(B6), 4281–4297.
McKenzie, D., Jackson, J., & Priestley, K. (2005). Thermal structure of oceanic and continental lithosphere. *Earth and Planetary Science Letters*, *233*(3–4), 337–349.
Mecklenburgh, J., & Rutter, E. (2003). On the rheology of partially molten synthetic granite. *Journal of Structural Geology*, *25*(10), 1575–1585.
Menegon, L., Pennacchioni, G., Malaspina, N., Harris, K., & Wood, E. (2017). Earthquakes as precursors of ductile shear zones in the dry and strong lower crust. *Geochemistry, Geophysics, Geosystems*, *18*, 4356–4374. https://doi.org/10.1002/2017GC007189
Mitchell, T. M., Toy, V., Di Toro, G., Renner, J., & Sibson, R. H. (2016). Fault welding by pseudotachylyte formation. *Geology*, *44*(12), 1059–1062.
Passchier, C. (1982). Pseudotachylyte and the development of ultramylonite bands in the saint-barthelemy massif, French pyrenees. *Journal of Structural Geology*, *4*(1), 69–79.
Paterson, M. (1990). Rock deformation experimentation. In A. G. Duba, W. B. Durham, J. W. Handin, & H. F. Wang (Eds.), *The brittle-ductile transition in rocks*. Geophysical Monograph Series (Vol. 56, pp. 187–194). Washington, DC: American Geophysical Union.
Pennacchioni, G., & Cesare, B. (1997). Ductile-brittle transition in pre-alpine amphibolite facies mylonites during evolution from water-present to water-deficient conditions (Mont Mary Nappe, Italian Western Alps). *Journal of Metamorphic Geology*, *15*(6), 777–791.
Platt, J., & Behr, W. (2011). Grainsize evolution in ductile shear zones: Implications for strain localization and the strength of the lithosphere. *Journal of Structural Geology*, *33*(4), 537–550.
Proctor, B., & Lockner, D. A. (2016). Pseudotachylyte increases the post-slip strength of faults. *Geology*, *44*(12), 1003–1006.
Rabinowitz, H., Skemer, P., Mitchell, T., & Di Toro, G. (2011). Experimental reactivation of pseudotachylyte-bearing faulted rocks. American Geophysical Union, Fall Meeting 2011 (T13A–2341).
Reilinger, R., Ergintav, S., Bürgmann, R., McClusky, S., Lenk, O., Barka, A., et al. (2000). Coseismic and postseismic fault slip for the 17 August 1999, m = 7.5, Izmit, Turkey earthquake. *Science*, *289*(5484), 1519–1524.
Rybacki, E., & Dresen, G. (2004). Deformation mechanism maps for feldspar rocks. *Tectonophysics*, *382*(3–4), 173–187.
Rybacki, E., Gottschalk, M., Wirth, R., & Dresen, G. (2006). Influence of water fugacity and activation volume on the flow properties of fine-grained anorthite aggregates. *Journal of Geophysical Research*, *111*, B03203. https://doi.org/10.1029/2005JB003663
Scholz, C. H. (1998). Earthquakes and friction laws. *Nature*, *391*(6662), 37–42.
Scholz, C. H. (2002). *The mechanics of earthquakes and faulting*. Cambridge, UK: Cambridge University Press.
Tokle, L., Hirth, G., & Behr, W. M. (2019). Flow laws and fabric transitions in wet quartzite. *Earth and Planetary Science Letters*, *505*, 152–161.
Trouw, R. A., Passchier, C. W., & Wiersma, D. J. (2009). *Atlas of mylonites-and related microstructures*. Berlin, Germany: Springer Science & Business Media.
Tse, S. T., & Rice, J. R. (1986). Crustal earthquake instability in relation to the depth variation of frictional slip properties. *Journal of Geophysical Research*, *91*(B9), 9452–9472.
Tullis, J., & Yund, R. (1992). The brittle-ductile transition in feldspar aggregates: An experimental study. *International Geophysics*, *51*, 89–117.
Violay, M., Gibert, B., Mainprice, D., Evans, B., Dautria, J.-M., Azais, P., & Pezard, P. (2012). An experimental study of the brittle-ductile transition of basalt at oceanic crust pressure and temperature conditions. *Journal of Geophysical Research*, *117*, B03213. https://doi.org/10.1029/2011JB008884
Watts, A., & Burov, E. (2003). Lithospheric strength and its relationship to the elastic and seismogenic layer thickness. *Earth and Planetary Science Letters*, *213*(1–2), 113–131.
Wright, T. J., Elliott, J. R., Wang, H., & Ryder, I. (2013). Earthquake cycle deformation and the Moho: Implications for the rheology of continental lithosphere. *Tectonophysics*, *609*, 504–523.